Contrasting patterns of phytoplankton pigments and chemotaxonomic groups along 30°S in the subtropical South Atlantic Ocean

Milton Luiz Vieira Araujo[a*], Carlos Rafael Borges Mendes[a],

Virginia Maria Tavano[a], Carlos Alberto Eiras Garcia[a], Molly O'Neil Baringer[b]

[a]Instituto de Oceanografia, Universidade Federal do Rio Grande, FURG, Rio Grande, RS 96203-900, BRAZIL

[b]Atlantic Oceanographic and Meteorological Laboratory, National Oceanic and Atmospheric Administration, NOAA, Miami, Florida 33149, USA

[*] Corresponding author: +55 53 32336746, araujomlv@gmail.com

Abstract

This work describes the spatial distribution of pigments and main taxonomic groups of phytoplankton in the biogeochemical provinces of the subtropical South Atlantic Ocean, along 30ºS latitude. Seawater samples (surface to 200 m depth) were collected along 120 oceanographic stations occupied in the early austral spring of 2011, during a CLIVAR Repeat Hydrography cruise. The pigments were identified and quantified by high performance liquid chromatography (HPLC), and CHEMTAX software was used to determine the relative contributions of the main taxonomic groups to total chlorophyll *a* (phytoplankton biomass index). Sampling stations were grouped into three provinces: Africa, Gyre and Brazil, corresponding to eastern, central and western sectors of the transect, respectively. Our results showed that both vertical and horizontal distribution patterns of pigments and taxonomic groups were mainly determined by the availability of light and/or nutrients. Photosynthetic carotenoids (PSCs), associated with small flagellates (mainly haptophytes), dominated the light-limited and nutrient-enhanced deep chlorophyll maximum (DCM) layers of both Brazil and Gyre provinces, as well as the upwelling influenced surface waters of the Africa province. The latter showed the highest chlorophyll *a* values (>1 $mg.m^{-3}$), and abundance of dinoflagellates in the coastal region. Photoprotective carotenoids (PPCs) were predominant at nutrient-poor and well lit surface layers of Brazil and Gyre provinces, associated with a low content of chlorophyll *a* (~ 0.1 $mg.m^{-3}$) and dominance of prokaryotes (*Synechoccocus* and *Prochloroccocus*). This study demonstrates the usefulness of using pigment analysis to better understand the distribution of phytoplankton communities along physical-chemical gradients in a still undersampled region of the South Atlantic Ocean.

Keywords: CLIVAR, phytoplankton community structure, biogeochemical provinces, HPLC, CHEMTAX

1. Introduction

Phytoplankton composition largely determines the trophic organization of pelagic ecosystems and thus the efficiency with which organic matter produced by photosynthesis is transferred towards upper trophic levels or exported to the deep ocean (Finkel et al., 2010). These primary producers are responsible for most of the carbon dioxide transfer from the atmosphere to the oceans and, consequently, play a fundamental role in the biogeochemical cycling of the planet, with different phytoplankton communities having specific biogeochemical roles (Schloss et al., 2007; Nair et al., 2008). To anticipate the effects of CO_2 on climate, the main recent earth system models are becoming increasingly complex and sophisticated in ocean ecology and biogeochemistry, incorporating complex modules of functional phytoplankton groups that drive marine biogeochemical cycles (Marinov et al., 2010). Thus, the study of phytoplankton communities provides a fundamental tool in environmental assessment and monitoring as well as in studies of trophic relationships and ecosystems modeling.

The distribution of phytoplankton in the oceans is governed primarily by the adaptation of communities to characteristic regional conditions such as turbulence, temperature, light and nutrients (Cullen et al., 2002). Longhurst et al. (1995) proposed a well-reasoned system for dividing the global ocean into biologically meaningful regions, evaluating patterns of productivity using ocean color data. These biogeochemical provinces are useful for comparing and contrasting biogeochemical processes and biodiversity between ocean regions (Oliver and Irwin, 2008). Nevertheless, the boundaries of these provinces are not fixed in time and space, but are rather dynamic and move according to seasonal and interannual changes in physical forcing (Longhurst, 2006). More recently, complementing this concept, Hooker et al. (2000) explored a vertical partitioning of the ocean into a near-surface mixed layer and a deep stratified layer. The two-layer approach is a consequence of

the importance of water column stability, which has a relevant effect on ocean biological production (Hooker et al., 2000). Horizontal partitioning of the oceans, which address the structure of phytoplankton communities, has been extensively used in several studies, but few of them have taken into account its vertical distribution.

Within this context, the South Atlantic Ocean (SAO) is one of the least investigated regions of the oceans and, thus, remains relatively poorly understood (Longhurst, 2006). The South Atlantic is particularly important as a region where oceanic properties are exchanged, mixed, and redistributed between different ocean basins. Moreover, it is the only major ocean basin that transports heat from the poles towards the equator (Talley, 2003). The SAO comprises an important part of the meridional overturning circulation (MOC), a worldwide wind- and buoyancy-driven transport that connects all basins and balances the global ocean energy flux (Garzoli et al., 2013). Additionally, the SAO is an important region where anthropogenic CO_2 penetrates into deep waters of the global oceans (Murata et al., 2008). The Atlantic Meridional Transect (AMT) Programme has greatly contributed to knowledge on biological processes in this ocean region (Aiken et al., 2000; Robinson et al., 2006). The AMT dataset includes a large set of observations on structure of phytoplankton communities (e.g., Gibb et al., 2000; Barlow et al., 2002, 2004; Poulton et al., 2006; Aiken et al., 2009). However, zonal east-west transects along the South Atlantic are very scarce. To fill this knowledge gap, the CLIVAR Repeat Hydrography Program (http://ushydro.ucsd.edu) aims to sample a set of hydrographic transects over the global ocean for obtaining high-quality measurements with a high resolution on spatial and vertical scales. A suite of physical and chemical parameters is determined throughout the water column to understand dynamics, interaction, and predictability of the coupled ocean-atmosphere system. The CLIVAR A10 section crosses the SAO at ~30°S, through the following biogeochemical provinces (as proposed by Longhurst et al., 1995): Benguela Current Coastal Province, South Atlantic

Gyral Province, and Brazil Current Coastal Province. Previous studies have already focused on phytoplankton community composition along this section; however, only surface data was investigated (Bouman et al., 2006, 2011; Barlow et al., 2007).

Accurate *in situ* measurements of phytoplankton composition are vital for advancing our understanding of the marine biogeochemistry, for instance, through development and validation of size-based phytoplankton biogeochemical models and remote-sensing algorithms (Brewin et al., 2014). Studies of phytoplankton community composition have been classically conducted using light microscope analysis, which is very time-consuming and requires a high level of taxonomic skill. An alternative way is through chemotaxonomic methods based on High Performance Liquid Chromatography (HPLC) pigment analysis (Mendes et al., 2015). These rely on the relative concentration of pigments that are characteristic of distinct algal taxonomic groups (Wright and Jeffrey, 2006; Higgins et al., 2011). A common approach involves using the software CHEMTAX (CHEMical TAXonomy) on HPLC pigment ratios signatures (Mackey et al., 1996) to determine the relative contribution of phytoplankton groups to total biomass. The HPLC-CHEMTAX approach has been successfully used in many worldwide investigations (e.g. Wright et al., 2010; Schlütter et al., 2011; Mendes et al., 2011, 2012, 2015) and provides valuable information about the whole phytoplankton community including small-size groups, which are normally difficult to identify by light microscopy. In the SAO, however, such studies have only been performed in coastal environments (Carreto et al., 2003, 2008; Rodrigues et al., 2014) and, consequently, the open ocean remains poorly explored with regard to phytoplankton communities.

The present work uses the HPLC-CHEMTAX approach to evaluate pigment data collected during the A10 section of the CLIVAR Repeat Hydrography Program. The study aims to increase our understanding on physical-chemical interactions that affect

phytoplankton communities (through pigment composition) at distinct provinces in the subtropical South Atlantic. The phytoplankton distribution patterns have been examined on both horizontal (along ~30°S) and vertical (between the surface and 200 m depth) scales. Within this context, the following specific questions have been posed: (1) How light and nutrient gradients affect the spatial distribution and composition of phytoplankton biomass? and (2) How does phytoplankton community structure changes with depth?

2. Material and Methods

2.1. Sampling and physical/chemical data

The CLIVAR A10 section in the SAO onboard NOAA Ship *Ronald H. Brown* was conducted during early austral spring 2011 (September 26 to October 31). This cruise was part of a decadal series of repeat hydrography sections jointly funded by NOAA-Climate Observations Division and NSF-OCE within the U.S. CLIVAR/CO2/hydrography/tracer program. The A10 section ran nominally along the 30°S from approximately 15°E to 50°W. A total of 120 full water column CTD/O_2/rosette (Seabird) casts were completed along the section, with nominal spacing between stations of ~30 nautical mile (nm) but at higher spatial resolution in the eastern and western boundaries (Fig. 1).

The study area was partitioned into three biogeochemical provinces, as proposed by Longhurst et al. (1995) and here denoted as Brazil, Gyre, and Africa provinces. The provinces' boundaries were determined by a cluster analysis (see Supplementary Material) using sea surface values of four selected environmental variables: temperature, salinity, dissolved oxygen, and total chlorophyll *a* (phytoplankton biomass index).

Physical and chemical data (temperature, salinity, oxygen, nutrients) were obtained from the online CLIVAR database (http://cchdo.ucsd.edu/cruise/33RO20110926). Nutrient analysis (nitrate, silicate, phosphate) was performed using the standard analysis protocol for

the WOCE hydrographic program (Gordon et al., 1993). The upper depth of the nitracline was determined from vertical profiles of nitrate concentration as the mean depth where nitrate concentration turn to a sharp gradient; this was generally observed as the depth below which nitrate concentrations exceeded 1 μmol.kg^{-1}. Seawater density (kg.m^{-3}) was determined from temperature, salinity, and pressure data to evaluate the stratification of water column. Upper mixed layer (UML) depth was determined as the depth at which potential density values were greater than 0.03 kg.m^{-3} from a near-surface value at 10 m depth (de Boyer Montégut et al., 2004). Water column stability (E) was estimated using vertical density variations, as a function of the buoyancy or Brunt-Väisälä frequency (N^2), which is defined by $N^2 = -(g/\rho).(\partial\rho/\partial z)$ (rad^2.s^{-2}), leading to $E = N^2/g$ (10^{-8} rad².m^{-1}), where g is gravity and ρ is the potential seawater density. Mean E values (between 0 and 100 m) were used in this study.

Photosynthetically active radiation (PAR; λ = 400–700 nm) in the upper 30 m layer was measured with a radiometric profiler (HyperPro, Satlantic) during 42 daytime sampling stations. The euphotic layer depth (Zeu), defined as the depth at which the downwelling irradiance of PAR falls to 1% of that just below the surface (Kirk, 2011), was estimated by using an exponential equation that describes the vertical attenuation of PAR: $I_z = I_0.\exp(-k.z)$, leading to Zeu = 4.6/k, where I is PAR (μmol.m^2.s^{-1}) and k is the attenuation coefficient (m^{-1}).

Seawater samples for phytoplankton pigment analysis were collected using Niskin bottles at three depths: surface (10 m), deep chlorophyll maximum (DCM), and below-DCM (where fluorescence levels stabilized at low values). The depths were selected according to the fluorescence profiles determined by an *in situ* fluorometer (ECO FL, WetLabs) coupled to the CTD system. Additionally, at some stations (numbered stations in Fig. 1), water samples were taken from several depths (between the surface and 200 m) to better characterize the vertical distribution of phytoplankton communities. A varying volume of seawater (1.5–3 L) was filtered in dim light onto Whatman GF/F filters (nominal pore size of 0.7 μm and 25 mm

diameter) using vacuum (pressure <5 in Hg) and immediately stored in liquid nitrogen for later HPLC pigment analysis.

2.2. HPLC pigment analysis

The filters were placed in a screw-cap centrifuge tube with 3 mL of 95% cold-buffered methanol (2% ammonium acetate) containing 0.05 mg L^{-1} trans-β-apo-8'-carotenal (Fluka) as internal standard. Samples were sonicated for 5 min in an ice-water bath, placed at –20ºC for 1h, and then centrifuged at 1100 rpm for 5 min at 3ºC. The supernatants were filtered through Fluoropore PTFE membrane filters (0.2 μm pore size), to rid the extract from remains of filter and cell debris. Immediately prior to injection, 1000 μL of sample was mixed with 400 μL of Milli-Q water in 2.0 ml glass sample vials, and these were placed in the HPLC cooling rack (4ºC). Methodological procedures for HPLC analyses (using a monomeric C8 column with a pyridine-containing mobile phase) are fully described in Zapata et al. (2000). The detection limit and quantification procedure of this method were conducted according to Mendes et al. (2007). Pigments were identified from both absorbance spectra and retention times from the signals in the photodiode array detector (SPD-M20A; 190–800 nm; 1 nm wavelength accuracy) or fluorescence detector (RF-10AXL; Ex. 430 nm/Em. 670 nm). Pigments were quantified from peak integration using LC-Solution software (Shimadzu), but all peak integrations were checked manually and corrected where necessary. The HPLC system was previously calibrated with pigment standards from DHI (Institute for Water and Environment, Denmark). The concentrations of pigments were normalized to the internal standard to correct for losses and volume changes. Table 1 list all pigments detected above the quantification limit and therefore analyzed in this study along with their respective abbreviations. The HPLC method presently used allowed separation of all pigments, except for chlorophyll *b* and divinyl-chlorophyll *b*, which exhibited the same retention time (co-elution) and, consequently, were presented together as Tchl *b*.

Pigment data were quality controlled according to Aiken et al. (2009). This quality control filter uses a linear relationship between accessory pigments (AP; all carotenoids plus chlorophylls *b* and *c*) and total chlorophyll *a* (Tchl *a*; the sum of monovinyl chlorophyll *a*, divinyl chlorophyll *a*, and chlorophyllide *a*) to either accept or eliminate specific samples. The rules for the quality control of the pigment data were: (1) The difference between Tchl *a* and AP should be less than 30% of the total pigment concentration (TP); (2) Regression analysis between Tchl *a* and AP should have a slope within the range 0.7–1.4 and must explain more than 90% of total variance ($r^2 > 0.9$). Our data showed a difference between Tchl *a* and AP always less than 30% of TP; and a regression between Tchl *a* and AP with a slope of 1.2 and $r^2 = 0.98$.

2.3. Photo-pigment indices

As phytoplankton may alter their pigment concentrations and composition in response to variations in irradiance intensity (Higgins et al., 2011), photo-pigment indices were derived according to Barlow et al. (2007) to assess the variation in contribution of Tchl *a* and carotenoids to the total pigment (TP) pool. Carotenoids were separated as photosynthetic (PSC) and photoprotective (PPC) (see Table 1 for pigments in each category). Accordingly, three photo-pigment indices were symbolised as Tchla_{TP}, PSC_{TP}, and PPC_{TP} and defined as given in Table 1. These indices were used to investigate the phytoplankton pigment adaptations in response to light environment regimes across the provinces and through the water column.

2.4. CHEMTAX analysis of pigment data

The relative contribution of microalgal groups to the overall biomass was calculated using CHEMTAX v1.95 chemical taxonomy software (Mackey et al., 1996) from the class-specific accessory pigments and total chlorophyll *a*. CHEMTAX uses a factor analysis and

steepest-descent algorithm to best fit the data onto an initial matrix of pigment ratios (ratio between respective accessory pigments and Tchl *a*). Procedures and calculations are fully described in Mackey et al. (1996).

The initial pigment ratios of major algal classes used here were compiled from Higgins et al. (2011) (see Supplementary Material), with chemotaxonomic groups being identified according to Jeffrey et al. (2011) (see Table 2). The same initial pigment ratio matrix was used on data from the three provinces (Brazil, Gyre, and Africa); however, data from each region were run separately to minimize potential variations in the CHEMTAX optimization procedures. Additionally, to account for variation of pigment ratios with irradiance and/or nutrient availability, these three datasets were further divided into three depth sets: 0–50 m samples, 50–100 m samples, >100 m samples (see Supplementary Material). Chl *a* was used for calculating the biomass of all groups, except *Prochlorococcus* , for which DV Chl *a* was used. A series of 60 pigment ratio matrices were generated by multiplying each ratio from the initial matrix by a random function to optimize the matrix, and 10% (n=6) of the generated ratios with lowest root-mean-square residual were averaged [see Wright et al. (2009) for further procedure details].

3. Results

3.1. Phytoplankton biomass and environmental conditions

The surface longitudinal variations in temperature, salinity, oxygen, and Tchl *a* clearly showed a strong gradient along the A10 section in the SAO, reflecting differences between the identified provinces in this study (Fig. 2). In the Africa province, a less saline (~35.5), oxygen-rich (>240 µmol.kg^{-1}), and cold (<18°C) surface water was observed, associated with relatively high Tchl *a* values (0.5-2 mg.m^{-3}). Contrarily, the Brazil province was characterized by warmer (>20°C), oxygen-poor (<230 µmol.kg^{-1}), and more saline

(>36.5) water, associated with low Tchl *a* levels (0.1–0.2 mg.m^{-3}). The Gyre province presented intermediate values of temperature, salinity, and oxygen (18-20°C, 35.5-36.5, 230-240 µmol.kg^{-1}, respectively), whereas Tchl *a* values were similar to that found in the Brazil province (~0.1 mg.m^{-3}). Mean values of physical-chemical properties at surface for each province are shown in Table 3. Despite low mean nutrient concentrations at surface in all provinces, the Africa region presented the highest values across the entire sampled region (Table 3). The mean N:P ratio was also very low at all stations. In the Africa province, the mean DCM depth was approximately coincident with the base of the UML and nitracline depth (~40 m), but shallower than the mean Zeu depth (~70 m). In the Brazil province, the upper layer showed the highest mean stability value (~400×10^{-8}.rad².m^{-1}) and the shallowest mean UML depth (~25 m). The mean DCM in the Brazil province was similar to Zeu depth (~85 m), but both shallower than the nitracline (~120 m). The Gyre province was characterized by the lowest mean stability value (~90×10^{-8}.rad².m^{-1}), an UML depth of about 50 m, and the deepest mean Zeu (~90 m) and nitracline (~130 m) depths.

In terms of vertical distribution of phytoplankton biomass (Fig. 3), highest Tchl *a* concentrations (mostly >1 mg.m^{-3}) were found at surface in the Africa province. In the Brazil province, Tchl *a* concentration at surface was low (~ 0.1-0.2 mg.m^{-3}), reaching a maximum of ~ 0.5 mg.m^{-3} at around 50-100 m. The Gyre province was characterized by low surface Tchl *a* concentrations (< 0.1 mg.m^{-3}), with an evident DCM (0.2–0.4 mg m^{-3}) around 100 m depth closely associated with the base of the euphotic layer and strongly coupled to the nitracline.

3.2. Phytoplankton pigments concentrations

A total of 21 phytoplankton pigments were identified in this study, and their concentrations at both surface and DCM layers reflect the distinct ocean regimes between the provinces (see Table 1). Highest mean pigment concentrations were found in the Africa province, with no significant differences between surface and DCM depth. The lowest mean pigment values were registered in the Gyre province. On the other hand, both the Gyre and Brazil provinces showed marked differences in pigment concentrations between surface and DCM depth. In the Africa province, Hex (haptophytes marker) was the main accessory pigment, with a mean concentration exceeding 100 $ng.L^{-1}$ and a significant contribution (~50 $ng.L^{-1}$) of Peri (dinoflagellates marker). The Brazil and Gyre provinces presented similar pigment composition patterns: DV Chl *a* (*Prochlorococcus* marker) was the main pigment at surface with a significant contribution of other accessory pigments (Chl *b*, But and Hex), typical pigment profile of the nanoflagellate-dominated plankton community, at DCM. A consistency of Zea (prokariotes marker) concentrations was observed along all provinces, both at surface and DCM layer, with values ~45−68 $ng.L^{-1}$.

3.3. Photo-pigment indices

Photo-pigment indices showed that Tchla_{TP} was relatively constant along the transect at both the surface and DCM layers, ranging between 0.4 and 0.5 (Fig. 4). PPC_{TP} at surface was relatively elevated (~0.3) in the Brazil and Gyre provinces, declining to low values (~0.1) in the Africa province. Contrarily, PSC_{TP} at surface was ~0.3 in the Africa province, declining to ~0.1 in both Brazil and Gyre provinces. At DCM depth, however, PPC_{TP} was always low (~0.1), while PSC_{TP} ranged between 0.2 and 0.3 along the study area.

3.4. Distribution of phytoplankton groups

In the Africa province, the community was dominated by flagellates (mainly Haptophytes-8) both at surface and DCM layers (Fig. 5). In both Brazil and Gyre provinces, however, the community was dominated by prokaryotes (*Synechococcus and Prochlorococcus*) at the surface and replaced by Haptophytes and *Prochlorococcus* at DCM depth. Diatoms and dinoflagellates, both at the surface and DCM depth, made a very small contribution to the phytoplankton community in most stations, except in the Africa province where Dinoflagellates increased in the coastal zone. It is important to note a low but consistent contribution of Prasinophytes and Pelagophytes along the DCM depth of all provinces.

Vertical distributions of phytoplankton groups (contributions to Tchl *a*) are shown for two selected and representative stations from each province (Fig. 6). In coastal waters of the Africa province (St. 1), the phytoplankton community was more diverse and abundant, and mainly composed of Dinoflagellates (~40%) and Haptophytes (~20%), with highest biomass values in the 0–40 m upper layer (Fig. 6a). In the oceanic zone of the Africa province (St. 12), phytoplankton diversity and abundance decreased. Dinoflagellates were almost absent, and Haptophytes emerged as the most important group (>40%), with a significant contribution of Pelagophytes (~20%), from the surface down to 150 m (Fig. 6b). In the Gyre province (St. 48 and St. 60), the phytoplankton community was mainly represented by *Synechococcus* and *Prochlorococcus* at the surface, while Haptophytes and *Prochlorococcus* appeared as the dominant groups at the DCM depth (Figs. 6c and 6d). In the Brazil province, a DCM depth was also evident but shallower depths than in the Gyre province. The oceanic waters of the Brazil province (St. 108) were dominated by *Synechococcus* and *Prochlorococcus* at the surface, while Haptophytes and *Prochlorococcus* appeared as the dominant groups at the DCM depth (Fig. 6e). In the coastal zone of the Brazil province

(St. 120), a great diversity of taxonomic groups was observed, with a significant contribution of Diatoms (~25%) at the surface, while Haptophytes, Prasinophytes, and Pelagophytes were observed at the DCM depth (Fig. 6f).

4. Discussion

Horizontal distribution of marine phytoplankton communities can be predicted to a certain extent by temperature and nutrients (Acevedo-Trejos et al., 2013), while light and nutrient availability, which can be affected by turbulence conditions, determine the phytoplankton distribution over depth (Cullen et al., 2002). The subtropical SAO sampled in this work encompasses biogeochemical provinces with distinct oceanographic regimes (deep ocean *vs.* coastal regions, upwelling zones, oligotrophic gyre), providing an ideal scenario for studying changes/adaptations of phytoplankton communities to distinct environmental conditions.

A considerable number of phytoplankton pigments have been detected in this work, and therefore, data reduction was necessary to extract the most relevant information on biogeochemical characteristics of the environment (Mendes et al., 2015). As expected, chlorophyll *a* was a major pigment in the studied phytoplankton communities, but Tchla_{TP} values were similar among the provinces (see Fig. 4 and Table1), demonstrating that the ratio Tchl *a*/total pigments was highly conservative, as suggested by Trees et al. (2000). This implies that accessory pigments play an important role on phytoplankton adaptive strategies to survive in the environment. Consequently, phytoplankton pigments and ratios (indices) can be used to determine changes in phytoplankton community structure and/or physiological responses to environmental settings. For instance, high concentrations of photosynthetic carotenoids (PSCs) normally indicate regions of high productivity and a dominance of large phytoplankton cells, whereas high photoprotective carotenoids (PPCs) proportions suggest

oligotrophic conditions associated with small phytoplankton cells (Gibb et al., 2000). On the other hand, it has been shown that phytoplankton communities accumulate more PPCs to mitigate cells photo-oxidative damage caused by high irradiance (PAR) levels and/or ultraviolet radiation (Moreno et al., 2012), whereas increases in PSCs are used to compensate light limitation (Rodríguez et al., 2006). In fact, in this study, highest proportions of PPCs were observed at surface nutrient-depleted waters of both Brazil and Gyre provinces, with a dominance of prokaryotes, indicating an oligotrophic condition (see Figs. 4 and 5). Inversely, flagellates (specifically dinoflagellates at coastal zone) were the dominant group at surface upwelling nutrient-rich waters of the Africa province. This pattern agrees well with previous phytoplankton pigment observations in SAO (Barlow et al., 2007; Aiken et al., 2009). At DCM depth, in turn, high proportions of PSC were found, associated with a clear dominance of flagellates (mainly haptophytes) along all provinces (see Figs. 4 and 5).

The DCM reflects a trade-off to phytoplankton communities exposed to two opposing resource gradients: nutrients supplied from below and light supplied from above (Huisman et al., 2006). Within this context, the distance between the nitracline and the base of the mixed layer highly affects vertical fluxes of nitrate in the ocean (Painter et al., 2008). For example, in subtropical gyres, there is a limited nutrient renewal at surface due to the nitracline being almost always deeper than the upper mixed layer (Neuer et al., 2007; Painter et al., 2008). This led some investigators to postulate the presence of two distinct layers within the euphotic zone: a well-mixed upper layer, where primary production is supported primarily by regenerated forms of nitrogen; and a lower layer, where production is predominately supported by new nutrients (primarily nitrate) that enter the euphotic zone (Painter et al., 2007), enhancing phytoplankton biomass and forming the DCM (Mignot et al., 2014). By controlling the metabolism *vs.* size-scaling relationship, nutrient supply plays a major role in determining community size structure and the energy flow through the pelagic ecosystems

(Marañón et al., 2007). Thus, nanoflagellate groups, as found mainly at DCM depths in this study (see Fig. 5), are expected to grow and dominate those deep environments. In fact, it has been reported that the nano size fraction of plankton is important in subtropical zones of the Atlantic (Tarran et al., 2006) and that a deep nanoflagellate population can develop close to the nitracline at very low light levels (Claustre and Marthy, 1995).

The southern Benguela area (co-located in this study with the Africa province) is a highly dynamic region influenced by local wind patterns that drive upwelling/relaxation cycles on timescales of days (Hutchings et al., 2009). A quasi-meridional front develops between recently cold-upwelled enriched waters at the coast and warmer oligotrophic offshore waters (Belkin et al., 2009). This strong cross-shore temperature gradient, coincident with the ambient nutrient concentrations, strongly influences the phytoplankton assemblages (Resende et al., 2007; Kudela et al., 2010). In general, the coastal upwelling communities are dominated by microplankton, the nearshore area by nanoplankton, and the offshore oceanic waters are mainly composed of prokariotes (picoplankton) (Fishwick et al., 2006; Hirata et al., 2009). Results presented here for the Africa province showed dinoflagellates to be the dominant group near the coast, responding to the upwelling signal and corresponding to the highest values of Chl *a*, while nanoflagellates (mainly haptophytes) appeared at intermediate environments (between nearshore and offshore) (see Fig. 6 a,b).

Subtropical ocean gyres are considered to be the marine analogues to terrestrial deserts because of chronic nutrient depletion and low standing stocks of organisms (Karl et al., 1995). While biological productivity within these oligotrophic regions may be relatively small, their contribution is significant to total production, due to the great surface dimension of the open oceans (McClain et al., 2004). In the present study, the Gyre province showed an upper mixed layer with almost undetectable nutrient levels and the presence of a DCM in the vicinity of the light-limited nitracline (see Table 3 and Fig. 3). Additionally, two distinct

vertical structures of pico-phytoplankton habitats were found for *Synechococcus* and *Prochlorococcus.* The first occupied surface waters, while the second was distributed throughout the water column with a subsurface maxima (see Figs. 5 and 6c,d), as also observed in Zubkov et al. (2000). *Prochlorococcus* can successfully inhabit the entire euphotic zone due to photoacclimation abilities of different ecotypes, physiologically and genetically distinct (Hickman et al., 2010). These ecotypes can be characterised by varying DVChl *b* to DVChl *a* ratios, indicating their adaptation to high-light (low DV Chl *b*/DV Chl *a* ratios) or low-light (high DV Chl *b*/DV Chl *a* ratios) environments (e.g., Carreto et al. 2008). In fact, in the present study, highest concentrations of Tchl *b* were detected at DCM of all provinces. Therefore, this pattern seems to be more associated with photoadaptation (and photoacclimation) processes occurring in different *Prochlorococcus* ecotypes than to the biomass of *Prochlorococcus* itself. The relative abundance of these ecotypes in the oceans is also related to changes in other environmental factors, like temperature, nutrients and vertical mixing dynamics (Bouman et al., 2006, 2011; Johnson et al. 2006, Zinser et al. 2007).

Haptophytes (e.g., coccolithophores) were an important group contributing to phytoplankton biomass in the Gyre at DCM depths (see Figs. 5 and 6c,d). Competition for light and nutrients strongly determines where and when Haptophytes will either flourish or fail (Gregg and Casey, 2007). These organisms have a slow growth and a fast sinking rate, but their low nitrate half-saturation constant and low light saturation for growth enable them to both efficiently utilize nutrients at reduced concentrations and effectively use low available irradiance. The key to success of these organisms in the global oceans is to find areas where nutrients and light are low enough to inhibit the growth of large groups (e.g. diatoms), but vertical mixing is high enough to prevent sinking losses and provide some nutrients from deep water masses (Gregg and Casey, 2007). Once thought to be homogeneous and static habitats, there is increasing evidence that oligotrophic gyres exhibit substantial physical and

biological variability on different time scales (McClain et al., 2004). Seasonal pulse events of new nutrients into the euphotic layer can occur due to deepening of mixed layer down to the nitracline (Cermeño et al., 2008). On the other hand, the relative position of the DCM depth in respect to nitracline migrate over seasonal timescales as a function of varying irradiances in the water column (Letelier et al., 2004; Mignot et al., 2014). The distinct mechanisms of light adaptation and nutrient tolerance of each phytoplankton group determines their relative dominance in this environment, as in the case of haptophytes found in this work.

In the Brazilian province, a prevalence of warm tropical water at surface sets a strong thermocline, separating deep nutrient-enriched waters from the euphotic zone, leading to a low productivity condition at surface (Brandini, 2006). In this region, most of biological energy in the surface layer comes from regenerated production from the constant recycling of nutrients by the microbial community, and an occasional rise in new production is fundamentally linked to seasonal processes of enrichment, such as local and small-scale upwelling events or continental river runoff (Metzler et al., 1997). In fact, it has been suggested that this region can be classified as “oligotrophic water with coastal influence” (Gonzalez-Silvera et al., 2004). However, due to a frequent oceanic intrusion of nutrient-rich water mass at the bottom layer on the continental shelf, the DCM is a typical oceanographic feature observed in this region and generally undetectable in remote sensing ocean color images (Brandini, 2006; Brandini et al., 2014). The DCM formation and community composition observed in the present study for this province (see Figs. 3 and 6e,f) agrees with previous studies (Odebrecht and Djurfeldt, 1996). The occurrence of this DCM is essential for the maintenance of pelagic and demersal fish resources in this region (Matsuura et al., 1996).

Near the Brazilian coast, the relatively low salinity at surface (see Fig. 2) is commonly observed due to influence of continental river runoff (Möller et al., 2008; Campos

et al., 2013). This relatively fresh and warm surface water mixed with bottom water of an incomplete upwelling stage can trigger a high stability and shallow UML (Lima et al., 1996) as observed in this study (see Table 3). However, the influence of this coastal water apparently did not affect phytoplankton biomass and community composition at surface. The low-biomass and prokaryote dominance at surface (see Fig. 6e,f) agrees with previous studies in this region (Brandini, 1990; Odebrecht and Djurfeldt, 1996; Gonzalez-Silvera et al., 2004; Garcia et al., 2005).

5. Conclusions

Phytoplankton biomass and community composition in the subtropical Atlantic Ocean varied according to distinct provinces along 30°S, and they were associated with distinct nutrient and light conditions. In the Africa province, due to influence of the Benguela upwelling system, highest Tchl *a* concentrations (>1 $mg.m^{-3}$) were found at surface, associated with a relatively shallow UML (0–50 m) and no evident DCM. The euphotic layer tended to be shallow, associated with high and homogeneously distributed nitrate concentrations in the entire water column. The community in this province was dominated by flagellates (mainly haptophytes and dinoflagellates in the coastal zone). In the Brazil province, the euphotic layer was relatively deep (75–100 m) with low surface nitrate concentrations (<1 $\mu mol.kg^{-1}$), which increased at depths below 50 m. Tchl *a* concentration at the surface was low (0.1-0.2 $mg.m^{-3}$), reaching a maximum of 0.5 mg m^{-3} at around 50-100 m. Towards the coast, lower salinity waters were associated with a diverse phytoplankton community, with important contributions of diatoms and various nanoflagellate groups at the surface and the DCM layers. The Gyre province was characterized by low surface Tchl *a* concentrations (<0.1 $mg.m^{-3}$), with an evident DCM around 100 m depth closely associated with the base of the euphotic layer and strongly

coupled to the nitracline. The community was dominated by prokaryotes, with two distribution patterns: while *Synechoccocus* was majorly found at the surface, *Prochloroccocus*) was abundant throughout the water column, sharing dominance with small flagellates (mainly haptophytes) at the DCM depth. At this layer, a significant enhancement in Tchl *b* concentration (also seen in the Brazil province) suggested the occurrence of distinct *Prochloroccocus* ecotypes, adapted to different light regime (surface vs. deep layers). The HPLC-CHEMTAX approach proved to be a powerful tool for mapping phytoplankton communities' distribution along the subtropical South Atlantic Ocean and also provided useful information on their physiological adaptations.

Acknowledgments

This study is a contribution to the activities of the Brazilian High Latitudes Oceanography Group (GOAL). GOAL has been funded by the Brazilian Antarctic Program (PROANTAR), the Brazilian Ministry of the Environment (MMA), the Brazilian Ministry of Science, Technology and Innovation (MCTI) and the Council for Research and Scientific Development of Brazil (CNPq). We thank captain and crew of the RV *Ronald H. Brown* and the NSF/ NOAA-funded U.S. CLIVAR Repeat Hydrography Program (funding provided by the NOAA Climate Program Office and the NOAA Atlantic Oceanographic and Meteorological Laboratory). We are very grateful to Simon Wright, from the Australian Antarctic Division, for providing CHEMTAX v.1.95, and to Luciano Azevedo for collecting all optical data and seawater samples for pigments analysis. M. L.V. Araujo and C.R.B. Mendes acknowledge financial support from the CAPES Foundation (Coordination for the Improvement of Higher Education Personnel). We are thankful for the constructive criticism of two anonymous reviewers, which helped to improve the manuscript.

References

Acevedo-trejos, E., Brandt, G., Merico, A., Smith, S.L., 2013. Biogeographical patterns of phytoplankton community size structure in the oceans. Global Ecology and Biogeography 22, 1060–1070.

Aiken, J., Rees, N., Hooker, S., Holligan, P., Bale, A., Robins, D., Moore, G., Harris, R., Pilgrim, D., 2000. The Atlantic Meridional Transect: overview and synthesis of data. Progress in Oceanography 45, 257–312.

Aiken, J., Pradhan, Y., Barlow, R., Lavender, S., Poulton, A., Holligan, P., Hardman-Mountford, N., 2009. Phytoplankton pigments and functional types in the Atlantic Ocean: A decadal assessment, 1995 – 2005. Deep-Sea Research II 56, 899–917.

Barlow, R.G., Aiken, J., Holligan, P.M., Cummings, D.G., Maritorena, S., Hooker, S., 2002. Phytoplankton pigment and absorption characteristics along meridional transects in the Atlantic Ocean. Deep-Sea Research I 47, 637–660.

Barlow, R.G., Aiken, J., Moore, G.F., Holligan, P.M., Lavender, S., 2004. Pigment adaptations in surface phytoplankton along the eastern boundary of the Atlantic Ocean. Marine Ecology Progress Series 281, 13–26.

Barlow, R., Lamont, T., 2012. Phytoplankton absorption and pigment adaptation of a red tide in the Benguela ecosystem. African Journal of Marine Science 34, 241–248.

Barlow, R., Stuart, V., Lutz, V., Sessions, H., Sathyendranath, S., Platt, T., Kyewalyanga, M., Clementson, L., Fukasawa, M., Watanabe, S., Devred, E., 2007. Seasonal pigment patterns of surface phytoplankton in the subtropical southern hemisphere. Deep-Sea Research I 54, 1687–1703.

Belkin, I.M., Cornillon, P.C., Sherman, K., 2009. Fronts in Large Marine Ecosystems. Progress in Oceanography 81, 223–236.

Bergkvist, J., Selander, E., Pavia, H., 2008. Induction of toxin production in dinoflagellates : the grazer makes a difference. Oecologia 156, 147–154.

Bouman, H.A., Ulloa, O., Barlow, R., Li, W.K.W., Platt, T., Zwirglmaier, K., Scanlan, D.J., Sathyendranath, S., 2011. Water-column stratification governs the community structure

of subtropical marine picophytoplankton. Environmental Microbiology Reports 3, 473–482.

Bouman, H.A., Ulloa, O., Scanlan, D.J., Zwirglmaier, K., Li, W.K.W., Platt, T., Stuart, V., Barlow, R., Leth, O., Clementson, L., Lutz, V., Fukasawa, M., Watanabe, S., Sathyendranath, S., 2006. Oceanographic basis of the global surface distribution of *Prochlorococcus* ecotypes. Science 312, 918-921.

Brandini, F.P., 1990. Hydrography and characteristics of the phytoplankton in shelf and oceanic waters off southeastern Brazil during winter (July/August1982) and summer (February/March1984). Hydrobiologia 196,111–148.

Brandini, F.P. 2006. Hidrografia e Produção Biológica na Região Sudeste-Sul do Brasil no Contexto do REVIZEE, in: Rossi-Wongtschowski, C.L.B., Madureira, L.S.M. (Eds.), O Ambiente Oceanográfico da Plataforma Continental e do Talude na Região Sudeste-Sul do Brasil, EDUSP, São Paulo, p. 459-466.

Brandini, F.P., Nogueira, M., Simião, M., Codina, J.C.U., Noernberg, M.A., 2014. Deep chlorophyll maximum and plankton community response to oceanic bottom intrusions on the continental shelf in the South Brazilian Bight. Continental Shelf Research 89, 61-75.

Brewin, R.J.W., Sathyendranath, S., Lange, P.K., Tilstone, G., 2014. Comparison of two methods to derive the size-structure of natural populations of phytoplankton. Deep-Sea Research I 85, 72–79.

Campos, P.C., Möller Jr, O.O., Piola, A.R., Palma, E.D., 2013. Seasonal variability and coastal upwelling near Cape Santa Marta. Journal of Geophysical Research: Oceans 118, 1–14.

Carreto, J.I., Montoya, N., Akselman, R., Carignan, M.O., Silva, R.I., Colleoni, D.A.C., 2008. Algal pigment patterns and phytoplankton assemblages in different water masses of the Río de la Plata maritime front. Continental Shelf Research 28, 1589–1606.

Carreto, J.I., Montoya, N.G., Benavides, H.R., Guerrero, R., Carignan, M.O.,2003. Characterization of spring phytoplankton communities in the Río de La Plata maritime front using pigment signatures and cell microscopy. Marine Biology 143, 1013–1027.

Cermeño, P., Dutkiewicz, S., Harris, R.P., Follows, M., Schofield, O., Falkowski, P.G., 2008. The role of nutricline depth in regulating the ocean carbon cycle. *Proceedings of the National Academy of Sciences* 105, 20344–20349

Claustre, H., Marty, J.C., 1995. Specific phytoplankton biomasses and their relation to primary production in the tropical North Atlantic. Deep-Sea Research I 42, 1475–1493.

Cullen, J.J., Franks, P.J.S., Karl, D.M., Longhurst, A., 2002. Physical influences on marine ecosystem dynamics, in: Robinson, A.R., McCarthy, J.J., Rothchild, B.J. (Eds.), The Sea, vol. 12. John Wiley & Sons, Inc., New York, pp. 297–336.

de Boyer Montégut, C., Madec, G., Fischer, A.S., Lazar, A., Iudicone, D., 2004. Mixed layer depth over the global ocean: An examination of profile data and a profile-based climatology. Journal of Geophysical Research 109, C12003.

de Souza, M.S., Mendes, C.R.B., Garcia, V.M.T., Pollery, R., Brotas, V., 2012. Phytoplankton community during a coccolithophorid bloom in the Patagonian shelf: microscopic and high-performance liquid chromatography pigment analyses. Journal of the Marine Biological Association of the United Kingdom 92, 13–27.

Finkel, Z.V., Beardall, J., Flynn, K.J., Quigg, A., Rees, T.A.V., Raven, J.A., 2010. Phytoplankton in a changing world: cell size and elemental stoichiometry. Journal of Plankton Research 32, 119–137.

Fishwick, J.R., Aiken, J., Barlow, R., Sessions, H., Bernard, S., Ras, J., 2006. Functional relationships and bio-optical properties derived from phytoplankton pigments , optical and photosynthetic parameters ; a case study of the Benguela ecosystem. Journal of the Marine Biological Association of the United Kingdom 86, 1267–1280.

Garcia, C.A.E., Garcia, M.V.T., McClain, C.R., 2005. Evaluation of SeaWiFS chlorophyll algorithms in the Southwestern Atlantic and Southern Oceans. Remote Sensing of Environment 95, 125–137.

Garcia, V.M.T., Garcia, C.A.E., Mata, M.M., Pollery, R.C., Piola, A.R., Signorini, S.R., McClain, C.R., Iglesias-Rodriguez, M.D., 2008. Environmental factors controlling the phytoplankton blooms at the Patagonia shelf-break in spring. Deep-Sea Research I 55, 1150–1166.

Garzoli, S.L., Baringer, M.O., Dong, S., Perez, R.C., Yao, Q., 2013. South Atlantic meridional fluxes. Deep-Sea Research I 71, 21–32.

Gibb, S.W., Barlow, R.G., Cummings, D.G., Rees, N.W., Trees, C.C., Holligan, P., Suggett, D., 2000. Surface phytoplankton pigment distributions in the Atlantic Ocean: an assessment of basin scale variability between 50°N and 50°S. Progress in Oceanography 45, 339–368.

Gibberd, M., Kean, E., Barlow, R., Thomalla, S., Lucas, M., 2013. Phytoplankton chemotaxonomy in the Atlantic sector of the Southern Ocean during late summer 2009. Deep-Sea Research I 78, 70–78.

Gonçalves-Araujo, R., de Souza, M.S., Mendes, C.R.B., Tavano, V.M., Pollery, R.C., Garcia, C.A.E., 2012. Brazil-Malvinas confluence : effects of environmental variability on phytoplankton community structure. Journal of Plankton Research 34, 399-415.

Gonzalez-Silvera, A., Santamaria-del-Angel, E., Garcia, V.M.T., Garcia, C.A.E., Millán-Nunes, R., Muller-Karger, F., 2004. Biogeographical regions of the tropical and subtropical Atlantic Ocean off South America : classification based on pigment (CZCS) and chlorophyll- a (SeaWiFS) variability. Continental Shelf Research 24, 983–1000.

Gordon, L.I., Jennings, J.C., Ross, A.A., Krest, J.M., 1993. A suggested protocol for continuous flow automated analysis of seawater nutrients (phosphate, nitrate, nitrite and silicic acid) in the WOCE Hydrographic Program and the Joint Global Ocean Fluxes Study. WOCE Operations Manual 3, 91-1.

Gregg, W.W., Casey, N.W., 2007. Modeling coccolithophores in the global oceans. Deep-Sea Research II 54, 447–477.

Gutiérrez-Rodríguez, A., Latasa, M., Mourre, B., Laws, E.A., 2009. Coupling between phytoplankton growth and microzooplankton grazing in dilution experiments : potential artefacts. Marine Ecology Progress Series 383, 1–9.

Hickman, A.E., Dutkiewicz, S., Williams, R.G., Follows, M.J., 2010. Modelling the effects of chromatic adaptation on phytoplankton community structure in the oligotrophic ocean. Marine Ecology Progress Series 406, 1–17.

Higgins, H.W., Wright, S.W., Schlüter, L., 2011. Quantitative interpretation of chemotaxonomic pigment data, in: Roy, S., Llewellyn, C.A., Egeland, E.S., Johnson, G. (Eds.), Phytoplankton Pigments: Characterization, Chemotaxonomy and Applications in Oceanography. Cambridge University Press, United Kingdom, pp. 257–313.

Hirata, T., Hardman-Mountford, N.J., Barlow, R., Lamont, T., Brewin, R., Smyth, T., Aiken, J., 2009. An inherent optical property approach to the estimation of size-specific photosynthetic rates in eastern boundary upwelling zones from satellite ocean colour: An initial assessment. Progress in Oceanography 83, 393–397.

Hooker, S.B., Rees, N.W., Aiken, J., 2000. An objective methodology for identifying oceanic provinces. Progress in Oceanography 45, 313–338.

Huisman, J., Thi, N.N.P., Karl, D.M., Sommeijer, B., 2006. Reduced mixing generates oscillations and chaos in the oceanic deep chlorophyll maximum. Nature 439, 322–325.

Hutchings, L., van der Lingen, C.D., Shannon, L.J., Crawford, R.J.M., Verheye, H.M.S., Bartholomae, C.H., van der Plas, A.K., Louw, D., Kreiner, A., Ostrowski, M., Fidel, Q., Barlow, R.G., Lamont, T., Coetzee, J., Shillington, F., Veitch, J., Currie, J.C., Monteiro, P.M.S., 2009. The Benguela Current: An ecosystem of four components. Progress in Oceanography 83, 15–32.

Johnson, Z.I, Zinser, E.R., Coe, A., McNulty, N.P., Woodward, E.M.S., Chisholm, S.W., 2006. Niche partitioning among *Prochlorococcus* phenotypes along ocean-scale environmental gradients. Science 311:1737–1740.

Karl, D.M., Letelier, R., Hebel, D., Tupas, L., Dore, J., Christian, J., Winn, C., 1995. Ecosystem changes in the North Pacific subtropical gyre attributed to the 1991-92 El Niño. Nature 373, 230-234.

Kirk, J.T.O., 2011. Light and Photosynthesis in Aquatic Ecosystems, third ed. Cambridge University Press, United Kingdom.

Kudela, R.M., Seeyave, S., Cochlan, W.P., 2010. The role of nutrients in regulation and promotion of harmful algal blooms in upwelling systems. Progress in Oceanography 85, 122–135.

Letelier, R.M., Karl, D.M., Abbott, M.R., Bidigare, R.R., 2004. Light driven seasonal patterns of chlorophyll and nitrate in the lower euphotic zone of the North Pacific Subtropical Gyre. Limnology and Oceanography 49, 508–519.

Lima I.D., Garcia, C.A.E., Möller, O.O., 1996. Ocean surface processes on the southern Brazilian shelf : characterization and seasonal variability. Continental Shelf Research 16, 1307–1317.

Longhurst, A., 2006. Ecological Geography of the Sea, 2nd ed., Academic Press, San Diego.

Longhurst, A., Sathyendranath, S., Platt, T., Caverhill, C., 1995. An estimate of global primary production in the ocean from satellite radiometer data. Journal of Plankton Research 17, 1245–1271.

Mackey, M.D., Mackey, D.J., Higgins, H.W., Wright, S.W., 1996. CHEMTAX- a program for estimating class abundances from chemical markers : application to HPLC measurements of phytoplankton. Marine Ecology Progress Series 144, 265–283.

Marañón, E., Cermeño, P., Rodríguez, J., Zubkov, M.V., Harris, R.P., 2007. Scaling of phytoplankton photosynthesis and cell size in the ocean. Limnology and Oceanography 52, 2190–2198.

Marinov, I., Doney, S.C., Lima, I.D., 2010. Response of ocean phytoplankton community structure to climate change over the 21st century: partitioning the effects of nutrients, temperature and light. Biogeosciences 7, 3941–3959.

Matsuura, Y., 1996. A probable cause of recruitment failure of the Brazilian sardine *Sardinella aurita* population during the 1974/75 spawning season. African Journal of Marine Science 17, 29–35.

McClain, C.R., Signorini, S.R., Christian, J.R., 2004. Subtropical gyre variability observed by ocean-color satellites. Deep-Sea Research II 51, 281–301.

Mendes, C.R., Cartaxana, P., Brotas, V., 2007. HPLC determination of phytoplankton and microphytobenthos pigments : comparing resolution and sensitivity of a C18 and a C8 method. Limnology and Oceanography: Methods 5, 363–370.

Mendes C.R.B., de Souza, M.S., Garcia, V.M.T., Leal, M.C., Brotas, V., Garcia, C.A.E., 2012. Dynamics of phytoplankton communities during late summer around the tip of the Antarctic Peninsula. Deep-Sea Research I 65, 1–14.

Mendes, C.R.B., Kerr, R., Tavano, V.M., Cavalheiro, F.A., Garcia, C.A.E., Dessai, D.R.G., Anilkumar, N., 2015. Cross-front phytoplankton pigments and chemotaxonomic groups in the Indian sector of the Southern Ocean. Deep-Sea Research II 118, 221–232.

Mendes C.R., Sá, C., Vitorino, J., Borges, C., Garcia, V.M.T., Brotas, V., 2011. Spatial distribution of phytoplankton assemblages in the Nazaré submarine canyon region (Portugal): HPLC-CHEMTAX approach. Journal of Marine Systems 87, 90–101.

Metzler, P.M., Glibert, P.M., Gaeta, S.A., Ludlam, J.M., 1997. New and regenerated production in the South Atlantic off Brazil. Deep-Sea Research I 44, 363–384.

Mignot, A., Claustre, H., Uitz, J., Poteau, A., D'Ortenzio, F., Xing, X., 2014. Understanding the seasonal dynamics of phytoplankton biomass and the deep chlorophyll maximum in oligotrophic environments: A Bio-Argo float investigation. Global Biogeochemical Cycles 28, 1–21.

Möller Jr., O.O., Piola, A.R., Freitas, A.C., Campos, E.J.D., 2008. The effects of river discharge and seasonal winds on the shelf off southeastern South America. Continental Shelf Research 28, 1607–1624.

Moreno, D.V., Marrero, J.P., Morales, J., García, C.L., Úbeda, M.G.V., Rueda, M.J., Llinás, O., 2012. Phytoplankton functional community structure in Argentinian continental shelf determined by HPLC pigment signatures. Estuarine, Coastal and Shelf Sciences 100, 72–81.

Murata, A., Kumamoto, Y., Sasaki, K., Watanabe, S., 2008. Decadal increases of anthropogenic CO 2 in the subtropical South Atlantic Ocean along 30°S. Journal of Geophysical Research 113, 1–16.

Nair, A., Sathyendranath, S., Platt, T., Morales, J., Stuart, V., Forget, M., Devred, E., Bouman, H., 2008. Remote sensing of phytoplankton functional types. Remote Sensing of Environment 112, 3366–3375.

Neuer, S., Cianca, A., Helmke, P., Freudenthal, T., Davenport, R., Meggers, H., Knoll, M., Santana-Casiano, J.M., González-Davila, M., Rueda, M., Llinás, O., 2007. Biogeochemistry and hydrography in the eastern subtropical North Atlantic gyre. Results from the European time-series station ESTOC. Progress in Oceanography 72, 1-29.

Odebrecht, C.,Djurfeldt,L.,1996. The role of nearshore mixing on phytoplankton size structure off Cape Santa Marta Grande, southern Brazil (Spring1989). Archive of Fishery and Marine Research 43(3), 217–230.

Oliver, M.J., Irwin, A.J., 2008. Objective global ocean biogeographic provinces. Geophysical Research Letters 35, 1–6.

Painter, S.C., Sanders, R., Poulton, A.J., Woodward, E.M.S., Lucas, M., Chamberlain, K., 2007. Nitrate uptake at photic zone depths is not important for export in the subtropical ocean. Global Biogeochemical Cycles 21, GB4005.

Painter, S.C., Sanders, R., Waldron, H.N., Lucas, M.I., Woodward, E.M.S., Chamberlain, K., 2008. Nitrate uptake along repeat meridional transects of the Atlantic Ocean. Journal of Marine Systems 74, 227–240.

Pitcher, G.C., Calder, D., 2000. Harmful algal blooms of the southern Benguela Current: a review and appraisal of monitoring from 1989 to 1997. African Journal of Marine Sciences 22, 255–271.

Pitcher, G.C., Nelson, G., 2006. Characteristics of the surface boundary layer important to the development of red tide on the southern Namaqua shelf of the Benguela upwelling system. Limnology and Oceanography 51, 2660–2674.

Poulton, A.J., Holligan, P.M., Hickman, A., Kim, Y., Adey, T.R., Stinchcombe, M.C., Holeton, C., Root, S., Woodward, E.M.S., 2006. Phytoplankton carbon fixation, chlorophyll-biomass and diagnostic pigments in the Atlantic Ocean. Deep-Sea Research II 53, 1593–1610.

Resende, P., Azeiteiro, U.M., Gonçalves, F., Pereira, M.J., 2007. Distribution and ecological preferences of diatoms and dinoflagellates in the west Iberian Coastal zone (North Portugal). Acta Oecologica 32, 224–235.

Robinson, C., Poulton, A.J., Holligan, P.M., Baker, A.R., Forster, G., Gist, N., Jickells, T.D., Malin, G., Upstill-goddard, R., Williams, R.G., Woodward, E.M.S., Zubkov, M. V, 2006. The Atlantic Meridional Transect (AMT) Programme: A contextual view 1995–2005. Deep-Sea Research II 53, 1485–1515.

Rodrigues, S. V, Marinho, M.M., Jonk C.C.C., Gonçalves, E.S., Brant, V.F., Paranhos, R., Curbelo, M.P., Falcão A.P., 2014. Phytoplankton community structures in shelf and oceanic waters off southeast Brazil (20^{o}–25^{o}S), as determined by pigment signatures. Deep-Sea Research I 88, 47–62.

Rodríguez, F., Chauton, M., Johnsen, G., Andresen, K., Olsen, L.M., Zapata, M., 2006. Photoacclimation in phytoplankton: implications for biomass estimates, pigment functionality and chemotaxonomy. Marine Biology 148, 963–971.

Schloss, I.R., Ferreyra, G.A., Ferrario, M.E., Almandoz, G.O., Codina, R., Bianchi, A.A., Balestrini, C.F., Ochoa, H.A., Pino, D.R., Poisson, A., 2007. Role of plankton communities in sea–air variations in pCO2 in the SW Atlantic Ocean. Marine Ecology Progress Series 332, 93–106.

Schlüter, L., Henriksen, P., Nielsen T.G., Jakobsen, H.H., 2011. Phytoplankton composition and biomass across the southern Indian Ocean. Deep-Sea Research I 58, 546–556.

Schoemann, V., Becquevort, S., Stefels, J., Rousseau, V., Lancelot, C., 2005. *Phaeocystis* blooms in the global ocean and their controlling mechanisms: A review. Journal of Sea Research 53, 43–66.

Selander, E., Jakobsen, H.H., Lombard, F., Kiørboe, T., 2011. Grazer cues induce stealth behavior in marine dinoflagellates. PNAS 108, 4030–4034.

Smayda, T.J., Trainer, V.L., 2010. Dinoflagellate blooms in upwelling systems: Seeding, variability, and contrasts with diatom bloom behaviour. Progress in Oceanography 85, 92–107.

Talley, L.D., 2003. Shallow, intermediate, and deep overturning components of the global heat budget. Journal of Physical Oceanography 33, 530–560.

Tarran, G.A., Heywood, J.L., Zubkov, M.V., 2006. Latitudinal changes in the standing stocks of nano- and picoeukaryotic phytoplankton in the Atlantic Ocean. Deep-Sea Research II 53, 1516–1529.

Ter Braak, C.J.F., Prentice, I.C., 1988. A theory of gradient analysis. Advances in Ecological Research 18, 271–317.

Trainer, V.L., Pitcher, G.C., Reguera, B., Smayda, T.J., 2010. The distribution and impacts of harmful algal bloom species in eastern boundary upwelling systems. Progress in Oceanography 85, 33–52.

Trees, C.C., Clark, D.K., Bidigare, R.R., Ondrusek, M.E., Mueller, J.L., 2000. Accessory pigments versus chlorophyll a concentrations within the euphotic zone : A ubiquitous relationship. Limnology and Oceanography 45, 1130–1143.

Wohlrab, S., Iversen, M.H., John, U., 2010. A molecular and co-evolutionary context for grazer induced toxin production in *Alexandrium tamarense*. *PLoS ONE* 5, e15039.

Wright, S.W., Ishikawa, A., Marchant, H.J., Davidson, A.T., van den Enden, R.L., Nash, G.V., 2009. Composition and significance of picophytoplankton in Antarctic waters. Polar Biology 797–808.

Wright, S.W., Jeffrey, S.W., 2006. Pigment markers for phytoplankton production, in: Volkmann, J.K. (Ed.), Marine Organic Matter: Biomarkers, Isotopes and DNA. Springer-Verlag, Berlin, pp. 71–104.

Wright, S.W., van den Enden, R.L., Pearce, I., Davidson, A.T., Scott, F.J., Westwood, K.J., 2010. Phytoplankton community structure and stocks in the Southern Ocean (30–80^{o}E) determined by CHEMTAX analysis of HPLC pigment signatures. Deep-Sea Research II 57, 758–778.

Zapata, M., Jeffrey, S.W., Wright, S.W., Rodriguez, F., Garrido, J.L., Clementston, L., 2004. Photosynthetic pigments in 37 species (65 strains) of Haptophyta: implications for oceanography and chemotaxonomy. Marine Ecology Progress Series 270, 83–102.

Zapata, M., Rodríguez, F., Garrido, J.L., 2000. Separation of chlorophylls and carotenoids from marine phytoplankton: a new HPLC method using a reversed phase C8 column and pyridine-containing mobile phases. Marine Ecology Progress Series 195, 29–45.

Zinser, E.R., Johnson, Z.I., Coe, A., Karaca, E., Veneziano, D., Chisholm, S.W., 2007. Influence of light and temperature on *Prochlorococcus* phenotype distributions in the Atlantic Ocean. Limnology and Oceanography 52:2205–2220.

Zubkov, M. V, Sleigh, M.A., Burkill, P.H., Leakey, R.J.G., 2000. Picoplankton community structure on the Atlantic Meridional Transect : a comparison between seasons. Progress in Oceanography 45, 369–386.

Table 1. Symbols, names, formulae, concentrations (in ng.L^{-1}) of pigments and pigment sums, and values of pigment indices identified in this study (mean ± standard deviation for each province at surface and DCM layer). Tchl *a* = total chlorophyll *a*, PPC = photoprotective carotenoids, PSC = photosynthetic carotenoids, AP = accessory pigments, TP= total pigments.

		Africa Province		Gyre Province		Brazil Province	
Symbol	**Description**	**Surface**	**DCM**	**Surface**	**DCM**	**Surface**	**DCM**
Chl *a*	Chlorophyll *a*	382.3 ± 405.9	457.8 ± 390.2	58.5 ± 23.3	194.1 ± 77.2	93.7 ± 45.4	268.3 ± 119.7
DV Chl *a*	Divinyl chlorophyll *a*	21.1 ± 15.1	46.6 ± 43.9	33.8 ± 15.8	90.4 ± 42.1	42.7 ± 10.1	125.5 ± 55.1
Tchl *b*	Chlorophyll *b* + Divinyl chlorophyll *b*	48 ± 42.8	77.5 ± 41	8.2 ± 6.5	90 ± 50.4	8.5 ± 4.4	108 ± 65
Chl c_2	Chlorophyll c_2	45.9 ± 57.9	63.9 ± 54.4	5 ± 2.8	25.1 ± 12.4	7.4 ± 4.5	27.5 ± 12.9
Chl c_3	Chlorophyll c_3	35 ± 26.4	58.2 ± 23.1	5.1 ± 3.2	42.2 ± 17.7	6.1 ± 3.5	47.3 ± 23.3
Fuco	Fucoxanthin	40.6 ± 45.1	58.7 ± 54.2	4.5 ± 3.9	16.3 ± 20.7	13.4 ± 10.5	15.5 ± 8.2
But	19'-butanoyloxyfucoxanthin	39 ± 20.2	65.3 ± 18.9	6.4 ± 3.2	50.6 ± 18.7	6.1 ± 2.6	53.1 ± 27.8
Hex	19'-hexanoyloxyfucoxanthin	104.3 ± 57.9	128.3 ± 65.7	14.9 ± 6.2	66.4 ± 25.8	16.3 ± 7.8	71.8 ± 28.9
Diad	Diadinoxanthin	38.5 ± 37.5	25.4 ± 38.4	4.1 ± 2.1	5.4 ± 2.4	6.2 ± 2.5	7.2 ± 2.5
Lut	Lutein	3.3 ± 1.9	3.2 ± 1.5	0.2 ± 0.4	1.4 ± 1.1	0.1 ± 0.2	1.8 ± 0.8
Pras	Prasinoxanthin	4.2 ± 6.4	5.4 ± 6.7	0.1 ± 0.4	2.3 ± 2	0.4 ± 0.7	6.5 ± 4.8
Allo	Alloxanthin	2.9 ± 5.3	3 ± 5	0 ± 0.2	0.8 ± 1.5	0.1 ± 0.2	2.7 ± 1.9
Diato	Diatoxanthin	3 ± 2.3	1.6 ± 1.6	0.3 ± 0.4	0.2 ± 0.3	0.7 ± 0.6	0 ± 0.1
Zea	Zeaxanthin	59.7 ± 36.2	67 ± 39.3	45.3 ± 11.2	43.8 ± 23.9	67.9 ± 10.3	62.7 ± 37.3
Car	βε-carotene + ββ-carotene	10.3 ± 9.8	14.4 ± 13.1	5.2 ± 2.5	16.4 ± 8.9	8.4 ± 3.9	25.2 ± 11.5
Peri	Peridinin	53.3 ± 166.4	56.4 ± 165.7	2.1 ± 4	3.7 ± 3.1	2.4 ± 0.7	4.9 ± 2.1
Viola	Violaxanthin	4.4 ± 3.6	4.4 ± 3.4	0.6 ± 0.4	1.3 ± 0.7	0.8 ± 0.4	1.4 ± 0.8
Pheide *a*	Pheophorbide *a*	7.1 ± 9.3	10.8 ± 8.6	1.4 ± 1.7	8.2 ± 4.7	1.9 ± 1.2	11.6 ± 6
Phe *a*	Pheophytin *a*	5.7 ± 6	8 ± 5.7	1.9 ± 1	6.8 ± 4.5	2.4 ± 1	8.3 ± 3.2
Chlide *a*	Cholophyllide *a*	3.5 ± 3.9	3.3 ± 3.9	0.1 ± 0.3	0.4 ± 0.9	0.5 ± 0.8	0.3 ± 0.3
Pigment sum							
Tchl *a*	Chl *a*+DVChl *a*+Chlide *a*	406.9 ± 402.2	507.7 ± 377.8	92.4 ± 35.1	284.9 ± 105.1	137 ± 45.6	394 ± 153.5
PPC	Viola+Diad+Allo+Diato+Zea+Car+Lut	122.2 ± 86.8	119 ± 86.9	55.7 ± 13.8	69.3 ± 32.1	84.3 ± 14.1	100.9 ± 48.6
PSC	But+Fuco+Hex+Peri+Pras	241.5 ± 272.6	314.1 ± 257.7	28 ± 13.4	139.3 ± 57.5	38.6 ± 20.7	151.7 ± 66.4
AP	PPC+PSC+Tchl *b*+Chl c_2+Chl c_3	492.5 ± 475.1	632.7 ± 437.8	102 ± 34.1	365.9 ± 143.4	144.9 ± 42.7	435.4 ± 183.5
TP	Tchl *a*+AP	899.5 ± 877	1140.3 ± 815.4	194.3 ± 68.8	650.8 ± 245.3	281.9 ± 87.9	829.4 ± 333.6
Photo-pigment index							
PPC_{TP}	PPC/TP	0.15 ± 0.03	0.1 ± 0.03	0.3 ± 0.04	0.11 ± 0.04	0.31 ± 0.05	0.12 ± 0.05
PSC_{TP}	PSC/TP	0.26 ± 0.03	0.27 ± 0.03	0.14 ± 0.03	0.21 ± 0.03	0.13 ± 0.03	0.19 ± 0.04
$Tchla_{TP}$	Tchl *a*/TP	0.45 ± 0.02	0.44 ± 0.01	0.47 ± 0.02	0.44 ± 0.03	0.48 ± 0.02	0.47 ± 0.04

Table 2. Chemotaxonomic groups and respective pigments used in CHEMTAX procedures.

Chemotaxonomic group	Pigments used in CHEMTAX
Prasinophytes	Chl *a*, Tchl *b*, Viola, Pras, Lut, Zea
Chlorophytes	Chl *a*, Tchl *b*, Viola, Lut, Zea
Cryptophytes	Chl *a*, Allo, Chl c_2
Diatoms-A	Chl *a*, Fuco, Chl c_2
Diatoms-B	Chl *a*, Fuco, Chl c_2, Chl c_3
Dinoflagellates	Chl *a*, Peri, Chl c_2
Haptophytes-6 (mainly coccolithophores)	Chl *a*, Fuco, Chl c_3, Hex, Chl c_2
Haptophytes-8 (mainly *Phaeocystis*)	Chl *a*, Fuco, Chl c_3, Hex, Chl c_2
Synechococcus	Chl *a*, Zea
Prochlorococcus	DV Chl *a*, Tchl *b*, Zea

Table 3. Mean ± standard deviation of environmental variables at surface (or water column for Zeu, DCM, MLD, Nitracline and E) for each province, in the study area.

	Africa Province	Gyre Province	Brazil Province
Temperature (^{o}C)	16.35 ± 0.77	18.34 ± 0.7	21.7 ± 0.97
Salinity	35.5 ± 0.22	36 ± 0.19	36.4 ± 0.65
Oxygen (µmol.kg^{-1})	248.62 ± 2.84	235.8 ± 4.71	220.76 ± 4.07
Nitrate (µmol.kg^{-1})	1.36 ± 1.68	0.02 ± 0.04	0.01 ± 0.03
Silicate (µmol.kg^{-1})	3.09 ± 1.93	1.13 ± 0.3	1.09 ± 0.86
Phosphate (µmol.kg^{-1})	0.28 ± 0.17	0.11 ± 0.05	0.07 ± 0.04
N:P	3.38 ± 2.84	0.17 ± 0.47	0.11 ± 0.43
Zeu depth (m)	70.8 ± 10.7	93.3 ± 9.9	88.1 ± 10.5
DCM depth (m)	43.8 ± 18.1	99.6 ± 22.5	82.2 ± 26.3
UML depth (m)	40.5 ± 19	52.8 ± 32.2	27.6 ± 14
Nitracline depth (m)	38.4 ± 29.3	128.9 ± 30.3	119.2 ± 55.4
E (10^{-8} rad^2.m^{-1})	142.4 ± 84.3	92.9 ± 72.2	400.5 ± 511.9

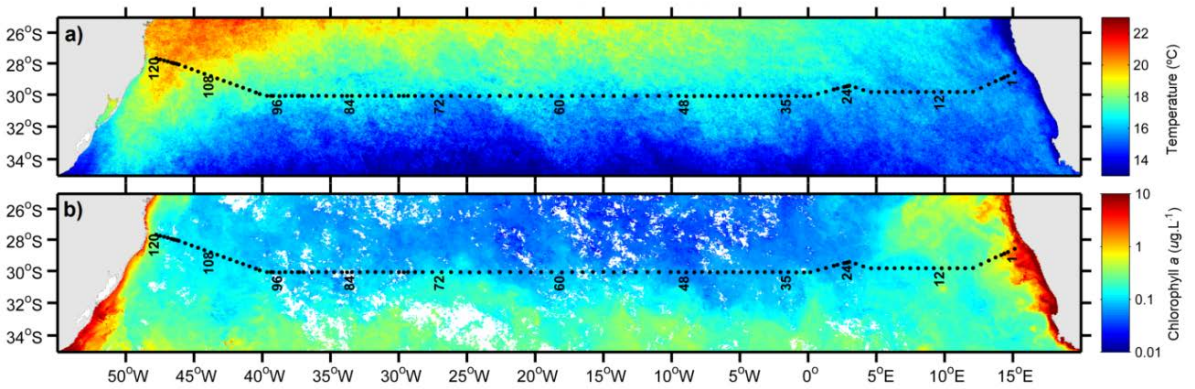

Fig 1. Satellite composite images of (a) sea surface temperature and (b) chlorophyll *a* for the cruise period (September 26–October 31, 2011) in the South Atlantic Ocean. Black dots indicate the stations' locations. Labelled stations indicate locations where high-resolution vertical pigments' profiles are available. Composite images were assembled from daily 4km resolution MODIS-Aqua satellite images.

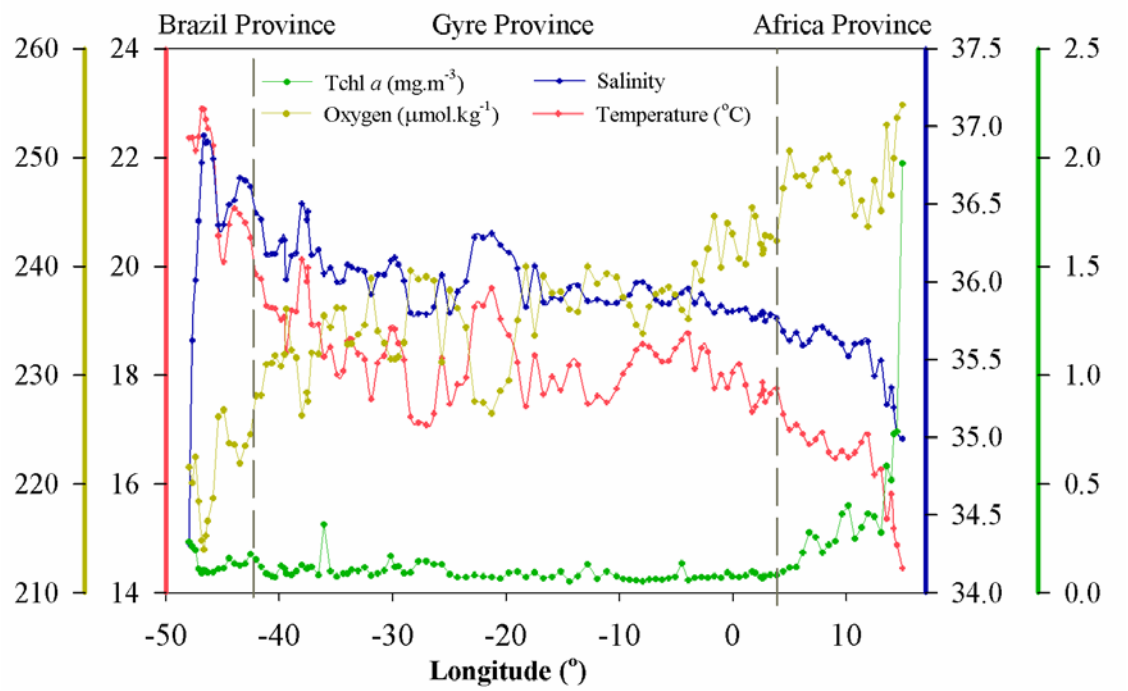

Fig 2. Surface longitudinal variation of selected variables (temperature, salinity, oxygen, and total chlorophyll *a*), used in the cluster analysis to define the three provinces in this study: Brazil, Gyre, and Africa provinces. Dashed lines indicate provinces' limits.

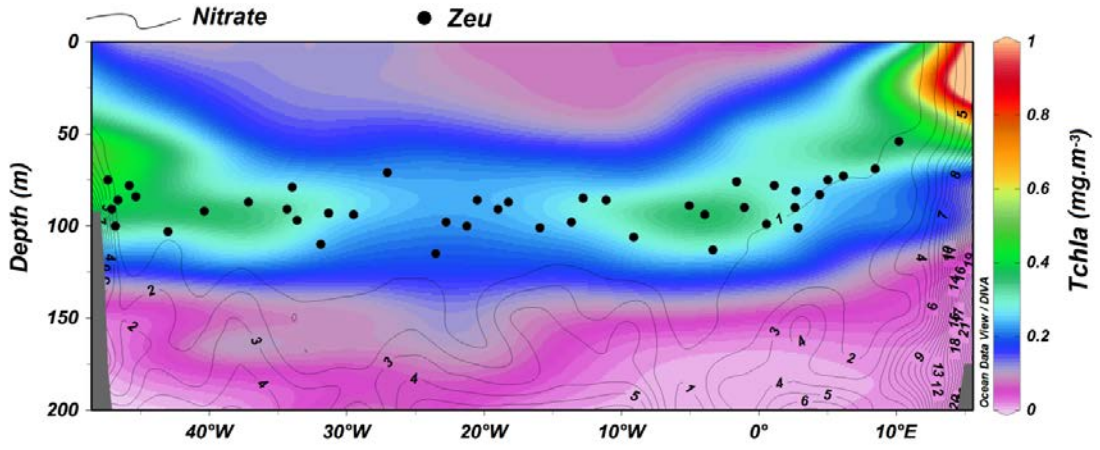

Fig 3. Vertical distribution of Tchl *a* along the 30°S transect. Contour lines indicate nitrate concentration (µmol.kg^{-1}). Black dots indicate the euphotic layer depth (Zeu).

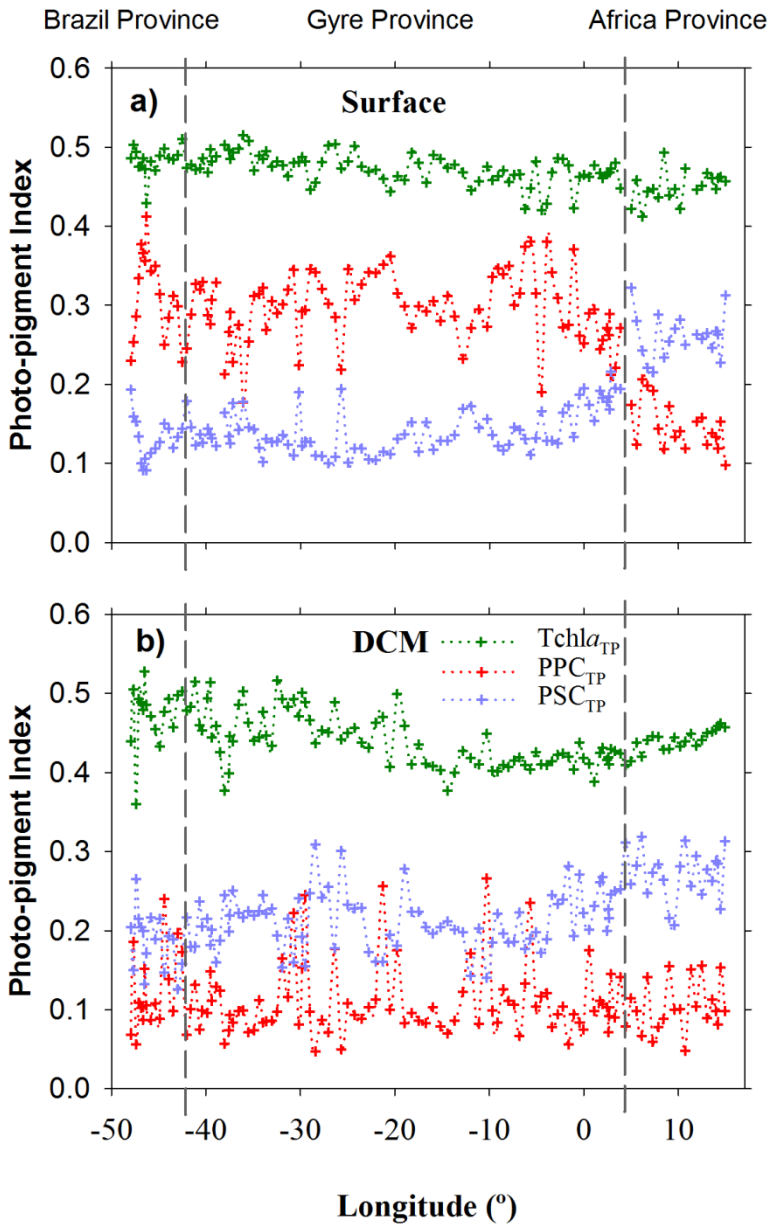

Fig 4. Longitudinal variations of Photo-pigment indices at (a) surface and (b) DCM depth in the study area. Tchla_{TP} = total chlorophyll *a* to total pigments, PPC$_{TP}$ = photoprotective carotenoids to total pigments, and PSC$_{TP}$ = photosynthetic carotenoids to total pigments. Dashed lines indicate the provinces' limits.

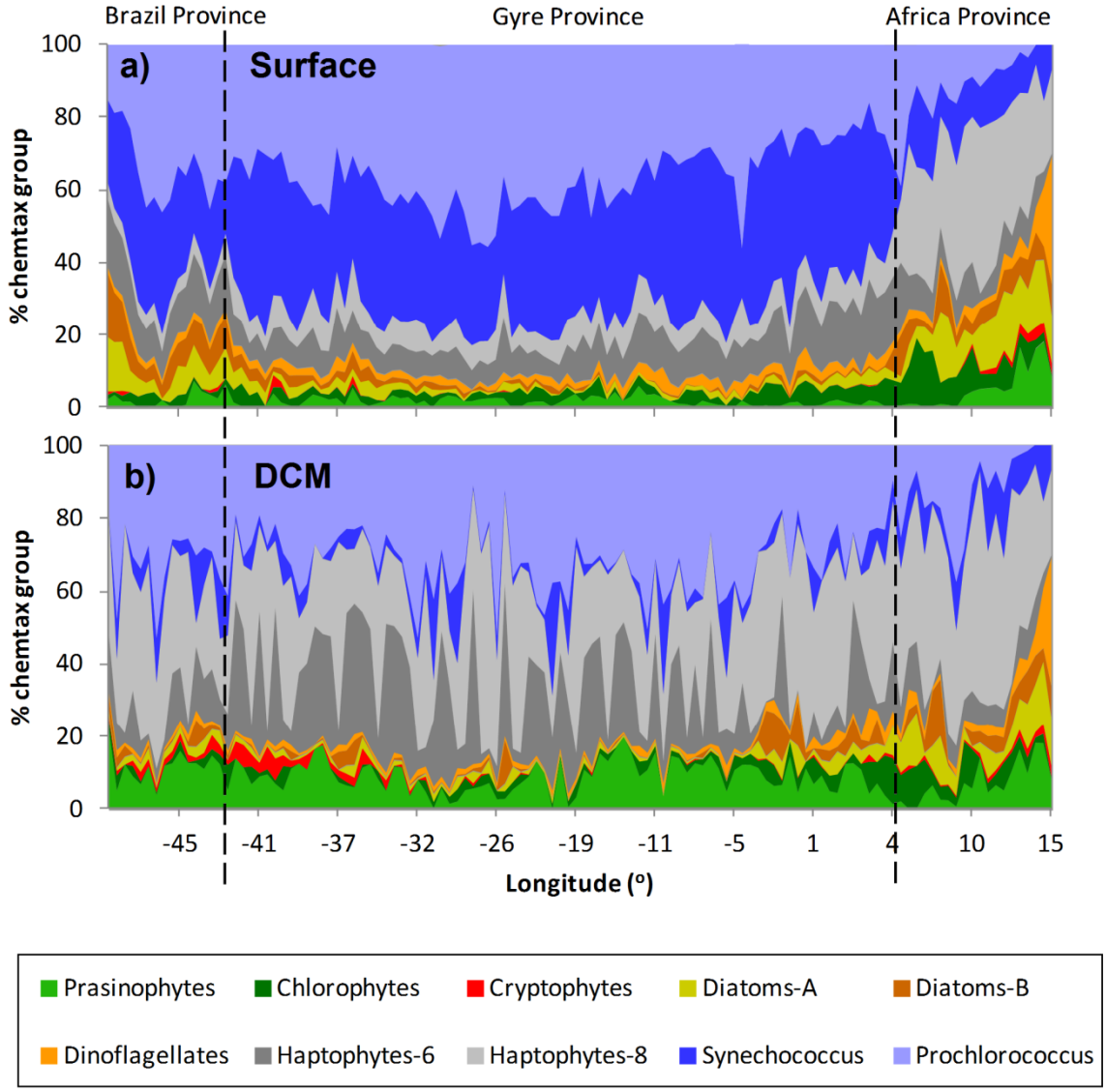

Fig 5. Longitudinal variations of phytoplankton groups (relative contributions to Tchl *a*) derived from CHEMTAX at (a) surface and (b) DCM depth in the study area. Dashed lines indicate the provinces' limits.

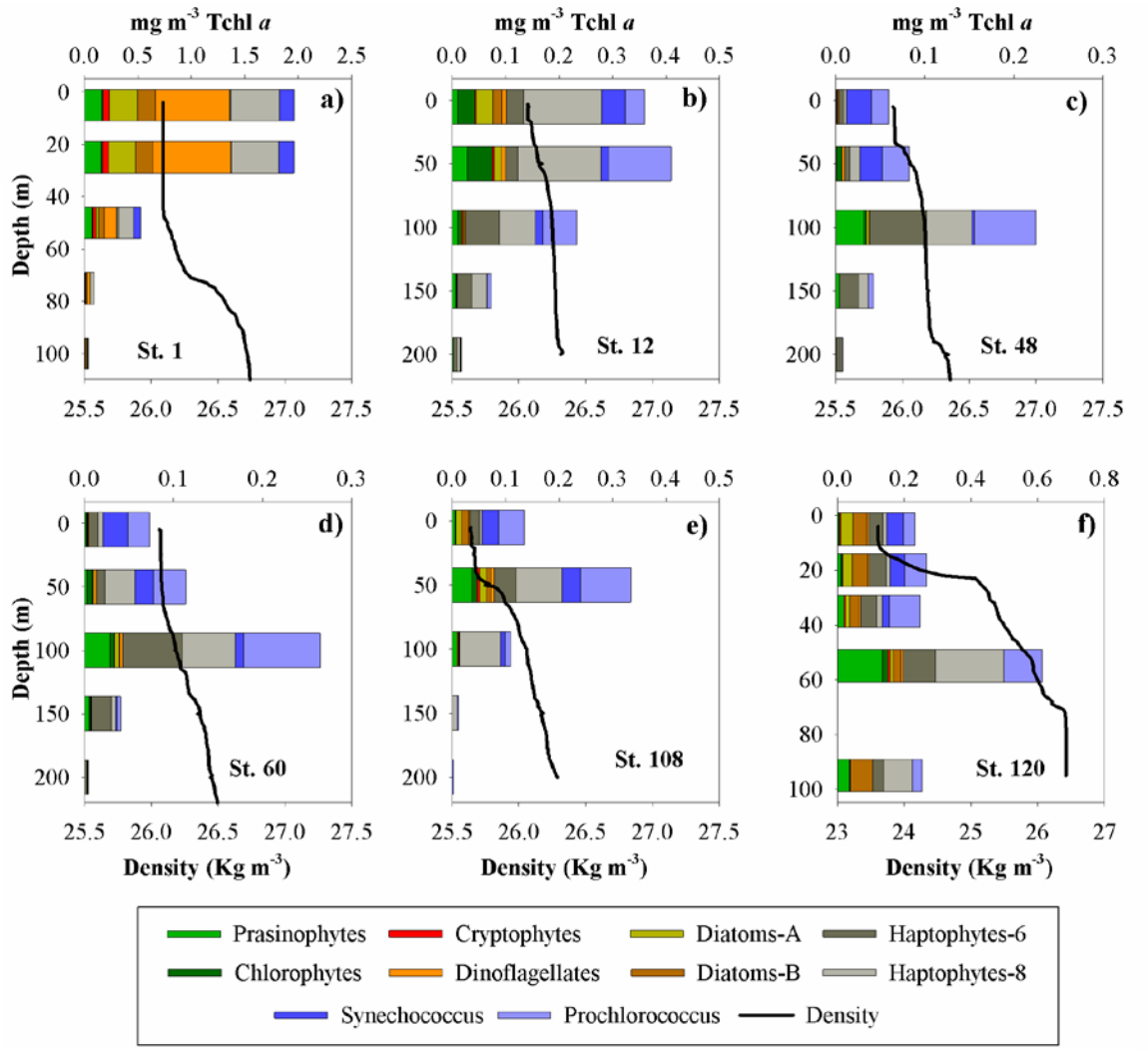

Fig 6. Vertical distribution of phytoplankton groups' biomass (as Tchl *a* concentration) derived from CHEMTAX at selected stations representative of each province identified in this study, and respective density profiles: (a,b) Africa province; (c,d) Gyre province; (e,f) Brazil province. Note the different scales.

Supplementary material

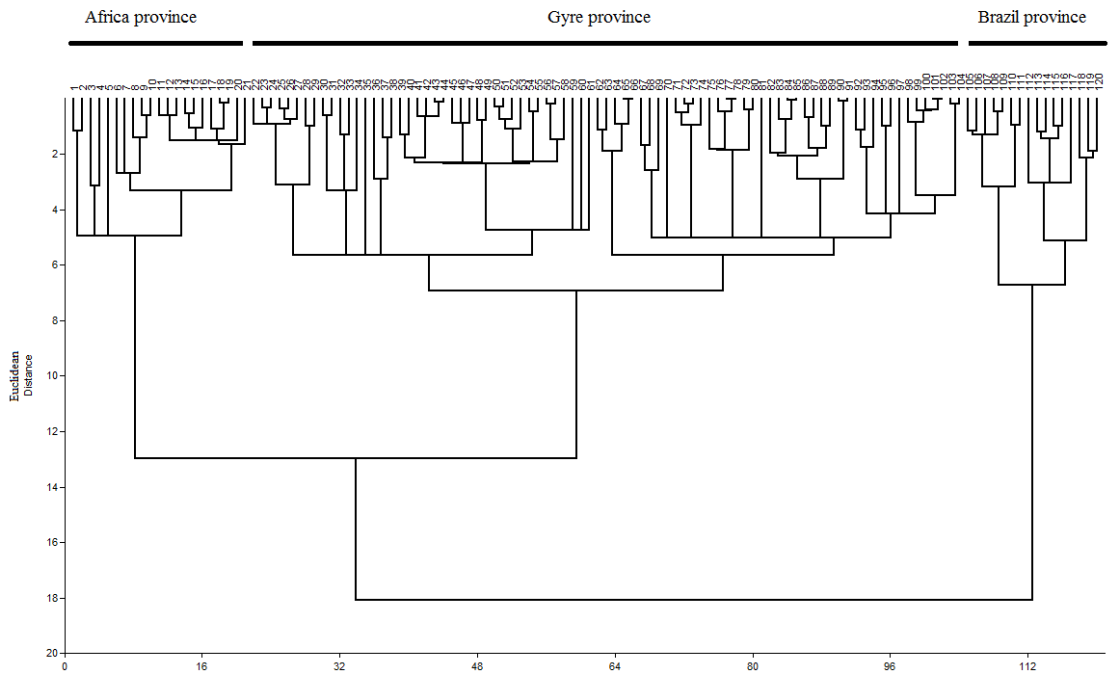

Fig. S1. Dendrogram of cluster analysis for sampling stations based on sea surface values (10m) of temperature, salinity, oxygen and total chlorophyll *a* using Euclidean distance similarity index and constrained linkage.

Table S1. Pigment ratios used in CHEMTAX analysis of pigment data: a) initial ratios before analysis, b) optimised ratios (for each province and depth) after analysis.

	Chl *a*	DV Chl *a*	Viola	Chl *c*$_2$	Fuco	Hex	Lut	Chl *c*$_3$	Pras	Allo	Zea	Peri	Tchl *b*
(a)Input matrix													
Prasinophytes	1	0	0.104	0	0	0	0.011	0	0.096	0	0.062	0	1.114
Chlorophytes	1	0	0.183	0	0	0	0.062	0	0	0	0.039	0	0.451
Cryptophytes	1	0	0	0.134	0	0	0	0	0	0.274	0	0	0
Diatoms-A	1	0	0	0.317	0.732	0	0	0	0	0	0	0	0
Diatoms-B	1	0	0	0.235	1.144	0	0	0.109	0	0	0	0	0
Dinoflagellates	1	0	0	0.258	0	0	0	0	0	0	0	0.848	0
Haptophytes-6	1	0	0	0.135	0.142	1.092	0	0.133	0	0	0	0	0
Haptophytes-8	1	0	0	0.368	0.249	0.763	0	0.286	0	0	0	0	0
Synechococcus	1	0	0	0	0	0	0	0	0	0	0.882	0	0
Prochlorococcus	0	1	0	0	0	0	0	0	0	0	0.287	0	0.322
(b) Output matrix													
Africa Province 0-50m													
	Chl *a*	DV Chl *a*	Viola	Chl *c*$_2$	Fuco	Hex	Lut	Chl *c*$_3$	Pras	Allo	Zea	Peri	Tchl *b*
Prasinophytes	1	0	0.076	0	0	0	0.012	0	0.146	0	0.074	0	0.936
Chlorophytes	1	0	0.095	0	0	0	0.141	0	0	0	0.043	0	0.51
Cryptophytes	1	0	0	0.16	0	0	0	0	0	0.417	0	0	0
Diatoms-A	1	0	0	0.091	0.398	0	0	0	0	0	0	0	0
Diatoms-B	1	0	0	0.306	1.248	0	0	0.129	0	0	0	0	0
Dinoflagellates	1	0	0	0.207	0	0	0	0	0	0	0	1.124	0
Haptophytes-6	1	0	0	0.153	0.177	1.911	0	0.106	0	0	0	0	0
Haptophytes-8	1	0	0	0.211	0.064	0.495	0	0.255	0	0	0	0	0
Synechococcus	1	0	0	0	0	0	0	0	0	0	1.254	0	0
Prochlorococcus	0	1	0	0	0	0	0	0	0	0	0.357	0	0.417
Africa Province 50-100m													
	Chl *a*	DV Chl *a*	Viola	Chl *c*$_2$	Fuco	Hex	Lut	Chl *c*$_3$	Pras	Allo	Zea	Peri	Tchl *b*
Prasinophytes	1	0	0.029	0	0	0	0.011	0	0.114	0	0.06	0	0.76
Chlorophytes	1	0	0.085	0	0	0	0.092	0	0	0	0.047	0	0.821
Cryptophytes	1	0	0	0.177	0	0	0	0	0	0.304	0	0	0
Diatoms-A	1	0	0	0.554	0.516	0	0	0	0	0	0	0	0
Diatoms-B	1	0	0	0.173	1.574	0	0	0.152	0	0	0	0	0
Dinoflagellates	1	0	0	0.159	0	0	0	0	0	0	0	1.006	0
Haptophytes-6	1	0	0	0.187	0.195	1.663	0	0.153	0	0	0	0	0
Haptophytes-8	1	0	0	0.143	0.053	0.313	0	0.318	0	0	0	0	0
Synechococcus	1	0	0	0	0	0	0	0	0	0	1.208	0	0
Prochlorococcus	0	1	0	0	0	0	0	0	0	0	0.313	0	0.648

Africa Province >100m

	Chl *a*	DV Chl *a*	Viola	Chl c_2	Fuco	Hex	Lut	Chl c_3	Pras	Allo	Zea	Peri	Tchl *b*
Prasinophytes	1	0	0.026	0	0	0	0.015	0	0.16	0	0.097	0	1.128
Chlorophytes	1	0	0.219	0	0	0	0.064	0	0	0	0.058	0	0.662
Cryptophytes	1	0	0	0.183	0	0	0	0	0	0.373	0	0	0
Diatoms-A	1	0	0	0.432	0.757	0	0	0	0	0	0	0	0
Diatoms-B	1	0	0	0.133	1.129	0	0	0.164	0	0	0	0	0
Dinoflagellates	1	0	0	0.154	0	0	0	0	0	0	0	0.946	0
Haptophytes-6	1	0	0	0.13	0.122	0.771	0	0.201	0	0	0	0	0
Haptophytes-8	1	0	0	0.219	0.162	0.809	0	0.3	0	0	0	0	0
Synechococcus	1	0	0	0	0	0	0	0	0	0	1.077	0	0
Prochlorococcus	0	1	0	0	0	0	0	0	0	0	0.202	0	0.885

Gyre Province 0-50m

	Chl *a*	DV Chl *a*	Viola	Chl c_2	Fuco	Hex	Lut	Chl c_3	Pras	Allo	Zea	Peri	Tchl *b*
Prasinophytes	1	0	0.063	0	0	0	0.015	0	0.043	0	0.077	0	1.678
Chlorophytes	1	0	0.237	0	0	0	0.072	0	0	0	0.036	0	0.459
Cryptophytes	1	0	0	0.158	0	0	0	0	0	0.268	0	0	0
Diatoms-A	1	0	0	0.483	0.694	0	0	0	0	0	0	0	0
Diatoms-B	1	0	0	0.257	1.599	0	0	0.14	0	0	0	0	0
Dinoflagellates	1	0	0	0.311	0	0	0	0	0	0	0	0.96	0
Haptophytes-6	1	0	0	0.152	0.107	1.12	0	0.179	0	0	0	0	0
Haptophytes-8	1	0	0	0.278	0.161	0.989	0	0.495	0	0	0	0	0
Synechococcus	1	0	0	0	0	0	0	0	0	0	1.036	0	0
Prochlorococcus	0	1	0	0	0	0	0	0	0	0	0.374	0	0.117

Gyre Province 50-100m

	Chl *a*	DV Chl *a*	Viola	Chl c_2	Fuco	Hex	Lut	Chl c_3	Pras	Allo	Zea	Peri	Tchl *b*
Prasinophytes	1	0	0.057	0	0	0	0.012	0	0.078	0	0.082	0	3.068
Chlorophytes	1	0	0.034	0	0	0	0.145	0	0	0	0.054	0	0.404
Cryptophytes	1	0	0	0.121	0	0	0	0	0	0.329	0	0	0
Diatoms-A	1	0	0	0.345	0.782	0	0	0	0	0	0	0	0
Diatoms-B	1	0	0	0.27	1.42	0	0	0.133	0	0	0	0	0
Dinoflagellates	1	0	0	0.408	0	0	0	0	0	0	0	0.846	0
Haptophytes-6	1	0	0	0.18	0.169	1.852	0	0.164	0	0	0	0	0
Haptophytes-8	1	0	0	0.156	0.041	0.418	0	0.316	0	0	0	0	0
Synechococcus	1	0	0	0	0	0	0	0	0	0	1.4	0	0
Prochlorococcus	0	1	0	0	0	0	0	0	0	0	0.339	0	0.141

Gyre Province >100m

	Chl *a*	DV Chl *a*	Viola	Chl c_2	Fuco	Hex	Lut	Chl c_3	Pras	Allo	Zea	Peri	Tchl *b*
Prasinophytes	1	0	0.022	0	0	0	0.017	0	0.066	0	0.076	0	2.483
Chlorophytes	1	0	0.251	0	0	0	0.036	0	0	0	0.045	0	0.566
Cryptophytes	1	0	0	0.139	0	0	0	0	0	0.344	0	0	0
Diatoms-A	1	0	0	0.432	0.946	0	0	0	0	0	0	0	0
Diatoms-B	1	0	0	0.241	1.209	0	0	0.095	0	0	0	0	0
Dinoflagellates	1	0	0	0.359	0	0	0	0	0	0	0	1.047	0
Haptophytes-6	1	0	0	0.058	0.06	0.613	0	0.167	0	0	0	0	0
Haptophytes-8	1	0	0	0.421	0.166	0.767	0	0.477	0	0	0	0	0
Synechococcus	1	0	0	0	0	0	0	0	0	0	1.193	0	0
Prochlorococcus	0	1	0	0	0	0	0	0	0	0	0.265	0	0.328

Brazil Province 0-50m

	Chl *a*	DV Chl *a*	Viola	Chl c_2	Fuco	Hex	Lut	Chl c_3	Pras	Allo	Zea	Peri	Tchl *b*
Prasinophytes	1	0	0.063	0	0	0	0.015	0	0.138	0	0.077	0	1.154
Chlorophytes	1	0	0.271	0	0	0	0.068	0	0	0	0.046	0	0.37
Cryptophytes	1	0	0	0.159	0	0	0	0	0	0.305	0	0	0
Diatoms-A	1	0	0	0.272	0.627	0	0	0	0	0	0	0	0
Diatoms-B	1	0	0	0.136	0.851	0	0	0.156	0	0	0	0	0
Dinoflagellates	1	0	0	0.231	0	0	0	0	0	0	0	1.027	0
Haptophytes-6	1	0	0	0.131	0.12	0.964	0	0.122	0	0	0	0	0
Haptophytes-8	1	0	0	0.384	0.328	0.831	0	0.348	0	0	0	0	0
Synechococcus	1	0	0	0	0	0	0	0	0	0	1.592	0	0
Prochlorococcus	0	1	0	0	0	0	0	0	0	0	0.372	0	0.099

Brazil Province 50-100m

	Chl *a*	DV Chl *a*	Viola	Chl c_2	Fuco	Hex	Lut	Chl c_3	Pras	Allo	Zea	Peri	Tchl *b*
Prasinophytes	1	0	0.018	0	0	0	0.011	0	0.141	0	0.071	0	1.799
Chlorophytes	1	0	0.054	0	0	0	0.094	0	0	0	0.049	0	0.545
Cryptophytes	1	0	0	0.151	0	0	0	0	0	0.397	0	0	0
Diatoms-A	1	0	0	0.431	0.688	0	0	0	0	0	0	0	0
Diatoms-B	1	0	0	0.052	1.074	0	0	0.099	0	0	0	0	0
Dinoflagellates	1	0	0	0.336	0	0	0	0	0	0	0	1.057	0
Haptophytes-6	1	0	0	0.187	0.111	1.212	0	0.187	0	0	0	0	0
Haptophytes-8	1	0	0	0.171	0.099	0.615	0	0.284	0	0	0	0	0
Synechococcus	1	0	0	0	0	0	0	0	0	0	1.086	0	0
Prochlorococcus	0	1	0	0	0	0	0	0	0	0	0.28	0	0.119

Brazil Province >100m

	Chl *a*	DV Chl *a*	Viola	Chl c_2	Fuco	Hex	Lut	Chl c_3	Pras	Allo	Zea	Peri	Tchl *b*
Prasinophytes	1	0	0.025	0	0	0	0.016	0	0.097	0	0.078	0	2.121
Chlorophytes	1	0	0.259	0	0	0	0.081	0	0	0	0.056	0	0.512
Cryptophytes	1	0	0	0.172	0	0	0	0	0	0.402	0	0	0
Diatoms-A	1	0	0	0.369	0.807	0	0	0	0	0	0	0	0
Diatoms-B	1	0	0	0.269	1.318	0	0	0.133	0	0	0	0	0
Dinoflagellates	1	0	0	0.31	0	0	0	0	0	0	0	1.09	0
Haptophytes-6	1	0	0	0.134	0.111	1.939	0	0.17	0	0	0	0	0
Haptophytes-8	1	0	0	0.102	0.032	0.32	0	0.308	0	0	0	0	0
Synechococcus	1	0	0	0	0	0	0	0	0	0	0.249	0	0
Prochlorococcus	0	1	0	0	0	0	0	0	0	0	0.278	0	0.305